Motion of phospholipidic vesicles along an inclined plane: Sliding and rolling

Manouk Abkarian, Colette Lartigue, and Annie Viallat*
Laboratoire de Spectrométrie Physique, UMR C5588 (CNRS), Université Joseph Fourier, Boîte Postale 87, 38402 Saint Martin d'Hères Cedex, France
(Received 15 September 2000; published 27 March 2001)

The migration of giant phospholipidic vesicles along an inclined plane in a quiescent fluid was observed as a function of the mass and the radius R of the vesicles, and as a function of the angle of inclination of the plane. Vesicles were swollen, and did not adhere to the substrate surface. It was observed from a side-view chamber that they have quasispherical shapes. The vesicles mainly slide along the plane, but also roll. The ratio $\omega R/v$ of rotational to translational velocities is of the order of 0.15 for vesicles of radius ranging from 10 to 30 μm. Values of this ratio, and variations of v versus R, are well described by Goldman *et al.*'s model developed for the motion of rigid spheres close to a wall [Chem. Eng. Sci. **22**, 637 (1967)]. In this framework, the thickness of the fluid film between the vesicle and the substrate derived from fitting experimental data was found to be equal to 48 nm.

DOI: 10.1103/PhysRevE.63.041906 PACS number(s): 87.16.Dg, 47.55.Dz

I. INTRODUCTION

This study is in keeping with the problem of migration and adhesion under external forces of membrane-bounded compartments occurring in biology, such as cells and transport vesicles. Such problems are of considerable biological importance, since cells migrate in tissues in response to forces induced by gradients of adhesion or gradients of concentration of chemoattractant moieties. They have generated many experimental observations of adhesion, sliding, and rolling of cells on functionalized substrates, generally under shear flow [1–3]. However, cell crawling is an extremely complex process involving mechanisms of the cell cytoskeleton like actin polymerization and gelation and specific interaction with the substrate [4–6]. Phospholipidic vesicles are more simple objects, whose membrane closely models biological membranes but which have no internal cytoskeleton. Vesicles are closed flexible lipid-bilayer membranes in suspension or which settle in aqueous solution. Despite their apparent simplicity, they have proven to be attractive model objects, since they can mimic shapes of cells and undergo ''cytolike'' processes including fusion, endocytosis, or adhesion [7,8]. Their equilibrium properties, such as shape phase diagram and membrane thermal fluctuations, have received much attention during the last decade [9] but their nonequilibrium properties have not been studied very much. Vesicle motion close to a wall is nevertheless far from trivial. Vesicles may adhere to the substrate or be repulsed due to the entropic contribution of membrane fluctuations. They can also be partially deflated, and present an excess of surface, which makes them easily deformable. Moreover, vesicle motion induces a coupling of the flow in the membrane to the surrounding bulk fluid. This last point was theoretically addressed recently [10–12]. Recently, the motion of adhering vesicles in a shear flow was reported which discloses a circular tanktreading motion of the vesicle, with a nonslip condition at the membrane surface [13].

The purpose of this paper is to describe the movement of spherical vesicles along an inclined plane in a quiescent fluid as a function of three physical quantities: vesicle mass, vesicle radius, and the tilting angle of the plane. The external driving force is gravity, and the substrate has no specific interaction with the vesicles. The first aim of this study is to find a theoretical framework for description of the observed motion. A framework was proposed by Goldman *et al.* to describe the motion of rigid spheres parallel to a plane wall in a viscous fluid, as a function of the separation distance between the sphere and the wall, δ, in the limit of small δ values [14]. The question which arises is whether this framework can be applied to deformable vesicles whose membrane is fluid, flickering, and highly permeable to water. The second aim is to determine the thickness δ of the thin fluid film under dynamic conditions. Little is known about the separation distance of vesicles and cells from the substrate. Reflection interference contrast microscopy (RICM) and fluorescence interferometry techniques provided the first measurements of this separation distance, but they concern only motionless objects [15,16].

The paper is organized as follows. After presentation of experimental aspects, the theoretical background for the motion of rigid spheres near a wall is briefly recalled in Sec. III. Then, the experimental shape of settled vesicles is described in Sec. IV. The translational motion of vesicles is analyzed in Sec. V. The rolling contribution is presented in Sec. VI. Results for the membrane-substrate separation distance are discussed in Sec. VII.

II. MATERIALS AND METHODS

A. Chemicals

All chemicals were purchased from Sigma: L-α phosphatidylcholine from fresh egg yolk (Egg-PC); sucrose and glucose, ''Sigma-ultra'' $>99.5\%$; bovine serum albumin; phosphate buffered saline tablets pH 7.4 at 25 °C. All sucrose and glucose solutions were prepared using ultrapure water (millipore quality).

*Email address: annie.viallat@ujf-grenoble.fr

B. Formation of vesicles

Giant vesicles were prepared from Egg-PC using the electroformation method [17]. We used a homemade preparation chamber composed of two transparent electrodes (glass plates coated with indium tin oxide) separated by a Teflon spacer (1 mm thick). The Egg-PC was dissolved in a mixture of chloroform and methanol (90:10 volume ratio) at a concentration of 0.5 mg/ml, and was spread on the conductive face of one of the two electrodes. After drying (1 h under vacuum), the chamber was assembled and filled with a sucrose solution. The ac voltage (10 Hz) was applied immediately, and the tension was progressively increased from 50 mV to about 1.5 V within 2 h. It was kept at 1.5 V for at least another hour. The frequency was finally decreased to 4 Hz to detach the vesicles from the glass plate. Vesicle solutions were stored at 8 °C. Four sucrose concentrations were used: 50, 100, 150, and 250 mM. Vesicle radii ranged from 10 to 70 μm.

C. Observation chambers

Two chambers were used. The first one was a parallelepiped-plate chamber (spectrophotometric circulation chamber from Hellma, $1\times10\times45$ mm^3). Optical observation was possible on its four quartz faces. The second one was a homemade parallel-plate chamber: two glass slides ($1\times26\times76$ mm^3), separated by a 1-mm-thick spacer, were tightened in a stainless steel outer frame. Nontreated slides were carefully washed and dried under argon (N treated). Some slides were subsequently dipped into a 90:10 mixture of sulphuric acid and hydrogen peroxide solution (30%) for 20 minutes (SP treated). Finally, some of these slides were immersed for 1 hour in a phosphate buffered solution (PBS; pH$=7.4$) containing 1 mg/ml bovine serum albumin (BSA treated) in order to prevent adhesion of vesicles on the substrate.

D. Microscope setup

Vesicles were observed using a phase contrast inverted microscope (Olympus IMT2). Most studies were done with a $10\times$ objective (Olympus, SPLAN, N.A$=0.30$). The microscope was installed on a rigid support which could be tilted using a graduated level up to an inclination of 15°. The observation chamber was fixed onto the microscope. Images were captured by a standard charged-coupled device camera (Burle, 1/2, USA) and digitized on an eight-bit frame grabber (Falcon Graphics, USA) installed on a Macintosh (acquisition software: Movie Machine, DigitalVision). Images of 388×284 pixels were analyzed with Image software (v1.62,NIH). With the $10\times$ objective, the pixel width was 1.17 μm.

E. Experimental method

1. Sample preparation

Well swollen vesicles were obtained by filling the observation chamber with a glucose solution whose concentrations (50, 101.8, 154, and 261 mM) equilibrate the osmolality of the sucrose solution inside the vesicles (concentrations of 50, 100, 150, and 250 mM, respectively). Then, from 20 to 50 μl of vesicle solution was gently added, and the chamber was tightly closed. The vesicle concentration was low enough to limit recirculation currents in the chamber, and to prevent undesirable coupling effects between vesicle movements.

2. Equilibration time

When the sucrose solution containing the vesicles is added to the glucose solution, vesicles slowly settle at the bottom of the chamber (sucrose is denser than glucose), and sucrose starts to diffuse within the chamber. The time required for a complete homogenization of the solution in the chamber is long, since diffusion processes are slow. When the chamber is inclined before complete homogenization of the glucose-sucrose solution, a recirculation current is generated, which introduces a bias in the determination of vesicle velocities, as will be shown in Sec. VI. This transient current progressively vanishes within a time of 10–20 min. Consequently, we always waited for at least 15 min to allow the settling of vesicles and homogenization of the fluids prior to starting measurements of translational velocities.

3. Measurements

For each measurement, isolated and well-contrasted vesicles were carefully chosen. The motion of each vesicle was first recorded at 0° inclination in order to estimate the magnitude and the direction of currents of thermal convection possibly present in the chamber.

Vesicle trajectories were then recorded at various inclinations (3°,6°,9°,12°, and 15°), starting from small angles and waiting for at least 10 min after each new inclination. The translation of one vesicle was recorded over a time ranging from 1 to 10 min, depending on its velocity and corresponding to a covered distance of the order of 400 μm (shot of the camera with the $10\times$ objective). For one vesicle, a complete measurement lasted 2–3 h; it was always done within 12 h after closing the observation chamber.

Rolling motion has been investigated through the observation of small defects ($1-5$ μm) either trapped within the lipid bilayer of the vesicle or simply bound to its internal part. Measurements were performed at 6° and 15°. The defect was going up and down during the movement, so that is had to be brought into focus during the time of measurement.

III. THEORETICAL BACKGROUND

The motion of a rigid sphere of radius R separated from a plane surface by a gap of width δ much smaller than R was theoretically treated by Goldman *et al.* [14] for low Reynolds numbers. From the Stokes equation, the force F and torque T exerted on the sphere may be written as the sum of the contribution of the viscous forces, due both to its translation parallel to the plane surface and its rotation. When δ/R is small, the lubrication theory yields

$$F=6\pi\eta Rv\left[\frac{8}{15}\ln\left(\frac{\delta}{R}\right)-0.9588\right]+6\pi\eta R^2\omega\left[-\frac{2}{15}\ln\left(\frac{\delta}{R}\right)-0.2526\right], \quad (1)$$

$$T=8\pi\eta R^2 v\left[-\frac{1}{10}\ln\left(\frac{\delta}{R}\right)-0.1895\right]+8\pi\eta R^3\omega\left[\frac{2}{5}\ln\left(\frac{\delta}{R}\right)-0.3817\right], \quad (2)$$

where v is the translational velocity, ω is the angular velocity, and η is the fluid viscosity. In the absence of external torque on the sphere, Eq. (2) leads to a relationship between rotational and translational velocities:

$$\frac{\omega R}{v}=\frac{\ln\left(\frac{\delta}{R}\right)+1.895}{4\ln\left(\frac{\delta}{R}\right)-3.817}. \quad (3)$$

In the case of a sphere moving under the influence of gravity, the force F is equal and opposite to the gravitational force on the sphere, corrected for the buoyancy of the fluid, and Eq. (1) writes as

$$\frac{4}{3}\pi R^3\Delta\rho\, g\sin\alpha=6\pi\eta Rv\left[\frac{8}{15}\ln\left(\frac{\delta}{R}\right)-0.9588\right]+6\pi\eta R^2\omega\left[-\frac{2}{15}\ln\left(\frac{\delta}{R}\right)-0.2526\right], \quad (4)$$

where α is the tilting angle of the plane, g is the acceleration of gravity, and $\Delta\rho$ is the volumic mass difference between sucrose and glucose solutions. For values of δ/R of the order of $5\times(10^{-4}-10^{-2})$ expected in this study (R varies from 5 to 70 μm and δ is expected to be in the range 10–100 nm), the second term on the right-hand side of Eq. (4) represents less then 2.5% of the first term, and can be neglected. Then the velocity v writes as

$$\frac{v}{\sin\alpha}=\frac{2}{9}\frac{\Delta\rho\, gR^2}{\eta}\left[\frac{8}{15}\ln\left(\frac{\delta}{R}\right)-0.9588\right]^{-1}. \quad (5)$$

Equation (5) allows one to derive the value of the separation distance δ from the measurements of R and v. Moreover, the measurement of the angular velocity [injected in Eq. (3)] permits one to test the validity of the model through the value of the ratio $\omega R/v$.

IV. VESICLE SHAPE

The profile of a vesicle in a meridian plane can be obtained from a side-view image. This was performed by tipping the microscope over at an angle of 90° (horizontal optical path) and using the four quartz faces (N-treated) chamber. This chamber was fixed onto the microscope with a special device. This permits one to incline the chamber perpendicularly to the optical path.

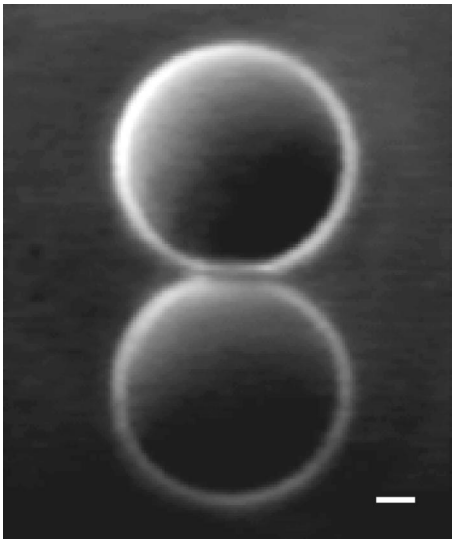

FIG. 1. Side view (upper) and reflected (lower) images of a vesicle of radius 36 μm prepared in a sucrose solution of concentration of 250 mM. The bar corresponds to 10 μm.

A typical picture is shown in Fig. 1 for a vesicle of 36-μm radius, settled at the bottom of the chamber at $\alpha=0°$. The vesicle profile and its image, reflected on the bottom face of the observation chamber, are clearly seen. The reflection facilitates a visualization of the contact zone between the vesicle and the quartz surface. The profile of the vesicle is a disk, almost nondeformed. It is only slightly flattened out at the bottom, due to gravity and the presence of the wall. The contact length is short (less than 10% of the circumference). These observations show that vesicles are quasispherical and, thus, nondeflated. We will show in the following that vesicles can indeed be satisfactorily described by spheres.

V. TRANSLATIONAL MOTION

In this section we present results for vesicle translational velocities. The resulting forces applied to the vesicles are controlled by varying two parameters: the tilting angle and the vesicle mass determined from the internal sucrose concentration. We establish a master curve of variations of a reduced variable determined by normalizing the translational velocity of a vesicle by its density, the tilting angle, and the bulk fluid viscosity, as functions of the vesicle radius.

The motion of 35 vesicles has been studied. Typical curves will be shown for two vesicles of radii equal to 19 and 52 μm, prepared at 150 and 250-mM sucrose concentrations, respectively, and referred as A and B vesicles in the following.

A. Trajectory analysis

Figure 2 shows trajectories of the center of mass of vesicles A [Fig. 2(a)] and B [Fig. 2(b)] observed for various tilting angles α. The direction of the steepest slope corresponds to the y axis. These trajectories are smooth and es-

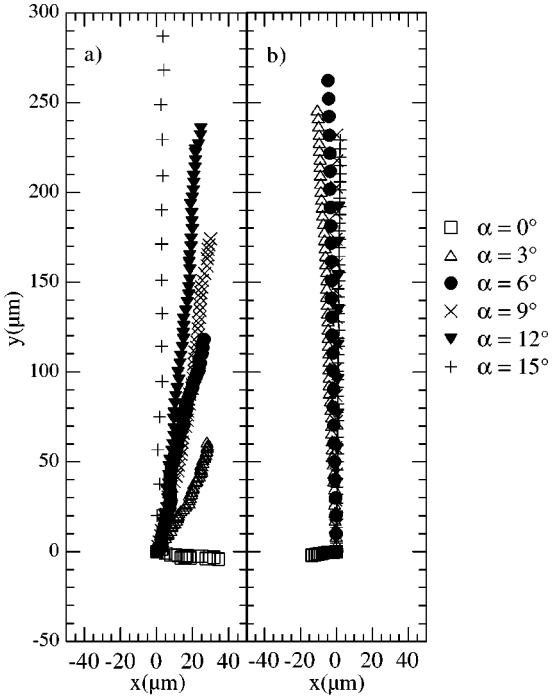

FIG. 2. Trajectories (a) and (b), respectively, for vesicles A and B (see text): α is the tilting angle, and the y axis is the axis of steepest slope. The motion at 0° is due to small thermal convection currents. The duration of measurements is 550 s for all trajectories of vesicle A; for vesible B, 550 s (0°,3°); 260 s (6°), 160 s (9°), and 100 s (12°,15°).

sentially linear, but their directions progressively change with the angle α. These deviations from the y axis are due to small thermal convection currents (also observable at $\alpha = 0°$). It clearly appears that the total motion results from the sum of effects due to gravitation and convection currents. Nevertheless, these latter effects, even for the strongest observed currents, were kept smaller than gravitational effects, at least for large angles. Figures 2(a) and 2(b) illustrate two cases where, on average, the effect of convection is large and small, respectively. Slight distortions of the trajectories have sometimes been observed due to the presence of surface defects, but they do not significantly affect the determination of vesicle velocities.

B. Velocities

The x and y coordinates of the center of mass of the vesicles are plotted versus time for each α value. Linear variations are observed, as shown in Fig. 3 for vesicle A, indicating that the velocity of vesicles is constant during a measurement. The values of the slopes of these curves are equal to translational velocities along x and y axes, respectively; $v_x(\alpha)$ and $v_y(\alpha)$. They range from 0.016 to 6.4 μm/s, depending on the size and mass of the vesicle.

For each vesicle, variations of $v_x(\alpha)$ and $v_y(\alpha)$ are plotted versus $\sin\alpha$, as illustrated in Fig. 4. Straight lines are clearly observed. They show that the velocities result from

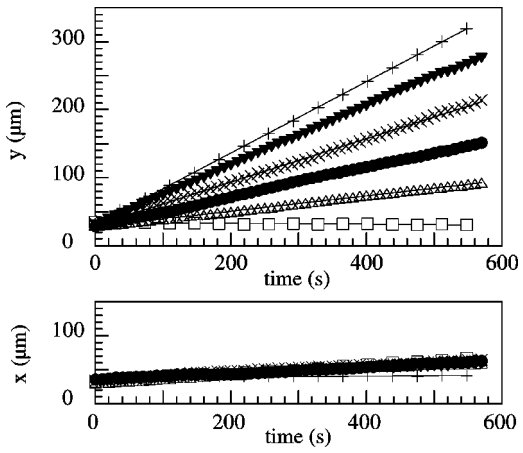

FIG. 3. Time variations of the coordinates of the center of mass of vesicle A. Same symbols as in Fig. 2. The slopes of the straight lines give $v_x(\alpha)$ and $v_y(\alpha)$.

two contributions. The relevant contribution, i.e., that induced by gravity, is $v/\sin\alpha$: $v_x(\alpha)/\sin\alpha$ and $v_y(\alpha)/\sin\alpha$ are determined from the slopes of the straight lines for $\alpha > 0°$. The second contribution, due to thermal convection currents, is characterized by the small nonzero values extrapolated on the curves at $\alpha = 0°$. They are typically of the order of 0.05 μm/s. These values represent the mean effect of convection currents, occurring during the time necessary for all measurements of one vesicle. Values of $v/\sin\alpha = [(v_x(\alpha)/\sin\alpha]^2 + \{[v_x(\alpha)/\sin\alpha]^2\}^{1/2}$ are reported in Table I together with vesicle radii, vesicle densities, and glass substrate treatments used for the measurements.

C. Master curve

On the basis of Eq. (5), we normalize the velocity by the fluid viscosity η, which varies with the glucose concentration, and by $\Delta\rho$, which depends on both the sucrose concentration in the vesicles and the glucose concentration in the external fluid. Then we plot the variation of the quantity

$$\frac{9\,\eta(v/\sin\alpha)}{2\Delta\rho g}$$

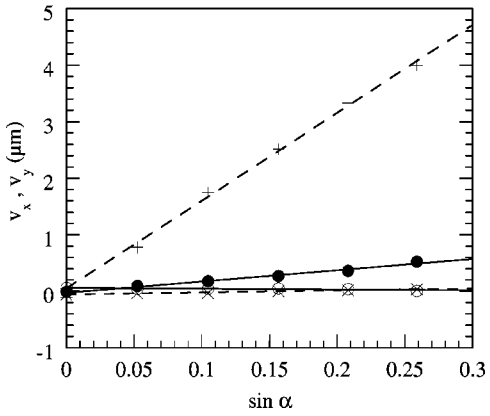

FIG. 4. Variations of $v_x(\alpha)$ and $v_y(\alpha)$ versus $\sin\alpha$ for vesicle A ($\bigcirc, v_x$; $\bullet, v_y$) and vesicle B ($\times, v_x$; $+, v_y$).

TABLE I. Experimemtal parameters (C_S's the sucrose concentration, and η_G and $\Delta\rho$ are the substrate treatments) and results for radii and velocities (ω_∞ measured at 15°) for all studied vesicles.

C_S (mM)	η_G (cP)	$\Delta\rho$ (g/l)	R (μm)	$v/\sin\alpha$ (μm/s)	ω_∞ (rad/s)	Substrate treatment
			14.7	0.3		N
			17.5	0.5		BSA
			17.7	0.5		BSA
			20.9	0.7		BSA
			22.1	0.9		SP
			22.3	0.9		BSA
50	1.017	3.2	22.8	1.1		N
			23.4	0.8		SP
			24.1	0.7		BSA
			26.7	1.2		BSA
			29.7	1.4		N
			29.8	1.4		SP
			30.3	1.2		N
			69	6.7		N
			37.3	5.1		SP
100	1.045	6.5	40	5.6		SP
			40	5.9		SP
			61.5	10.0		SP
			10.4	0.4		SP
150	1.074	9.9	17.2	1.5		SP
Vesicle A			19.2	1.9		SP
			20.6	3.0		SP
			13.5	1.5	0.0050	SP
			15.2	0.9		SP
			18	2.1		SP
			22.5	3.7		SP
			24	3.6		SP
			31	5.8		SP
250	1.133	16	33.5	5.4	0.0053	SP
			34.4	7.8		N
			35	8.2		SP
			45.3	10.0		SP
			45.8	15.4		SP
Vesicle B			51.6	16.0		N
			57.8	24.6		SP

versus R^2 (Fig. 5). All points obtained from four different sucrose concentrations lie on a single curve independently of the substrate treatment. As BSA-covered glass is a nonadhesive surface, the two other substrates are also considered nonadhesive. Adhesion forces are therefore nonrelevant in this study, and one expects the model developed for rigid spheres to be valid as long as membrane fluctuations and water permeability do not significantly affect the hydrodynamic behavior. Experimental data are fitted using Eq. (5) with a single adjustable parameter δ, the distance between the membrane and the substrate. A very good agreement is observed as shown in Fig. 5, yielding $\delta = 48$ nm.

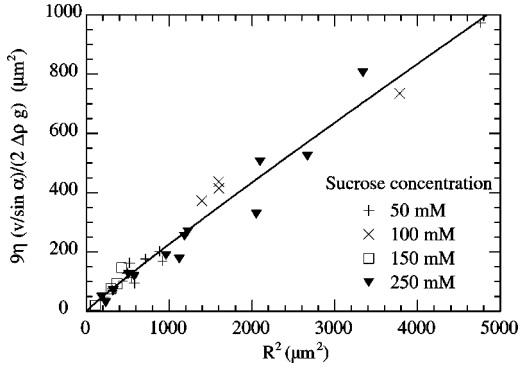

FIG. 5. Variations of $9\eta(v/\sin\alpha)/(2\Delta\rho g)$ vs R^2 (see text). The points have been obtained from three different substrates (N, SP, and BSA treated; see Table I). The curve is a fit of Eq. (5) (Goldman *et al.*'s model) with $\delta = 48$ nm.

VI. ROLLING MOTION

We further investigated the movement of vesicles and tested the validity of Goldman *et al.*'s model by exploring the rolling motion. For practical reasons, rolling motion measurements were performed rapidly after preparation of the observation chamber, i.e., before fluid homogenization in the chamber (see Sec. II). Consequently, angular and translational velocities decrease with time during the recordings. In this section, we first analyze the motion of a defect bound to the membrane over time intervals short enough so that velocities can be considered constant. Then we study in detail the decay of the velocities of two vesicles until the stationary regime is reached. Angular velocities are determined and Goldman *et al.*'s model is tested through Eq. (3).

A. Characterization of the rolling motion

Rolling motion was observed for large tilting angles (6° or 15°) in order to reduce the effect of convection currents. The trajectories of the center of mass of the studied vesicles were linear. The positions (relative to that of the center of mass of the vesicles) of the defects bound to the vesicles, x_d and y_d, were plotted as a function of time. This is shown in Fig. 6 for a defect of radius $r_d \approx 5$ μm bound to a vesicle of radius $R = 32$ μm. An oscillatory behavior characteristic of a rolling motion is observed for y_d while x_d remains constant. This indicates that the x axis is the axis of rotation of the vesicle; it is horizontal and perpendicular to the direction of motion. For a spherical vesicle, the defect in the membrane is expected to exhibit a circular motion of radius $\varrho = [(R - r_d)^2 - x_d^2]^{1/2}$ in a vertical plane perpendicular to the x axis, leading to a sinusoidal variation of y_d versus time. A sinusoid of equation $y_d = \varrho \sin(\omega t + \phi)$ is indeed superimposed on the data in Fig. 6. It fits the data quite well, although an asymmetry of the experimental curve is observed. The fit can be improved by adding a small periodical correction to the argument $y_d = \varrho \sin[\omega t + \phi + \epsilon \sin(\omega t) + \epsilon' \cos(\omega t)]$. As seen in Fig. 6, this correction remains small. This asymmetry may be understood as originating from the stationary shape of the vesicle, which deviates slightly from the spherical shape. As shown by this example, the variation of the

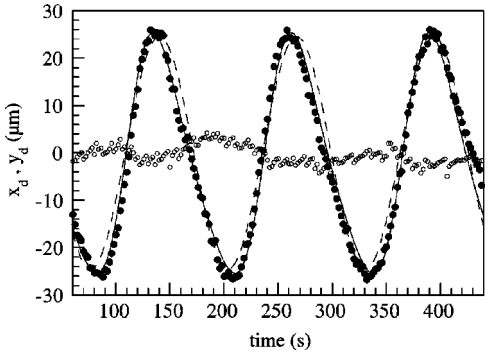

FIG. 6. Motion of a defect bound to a vesicle ($R=32$ μm) running down an inclined plane in the y direction ($\alpha=15°$): y_d (●) is the relative position with respect to the center of mass of the vesicle. The defect is in the vertical plane perpendicular to the axis of rotation, and containing the center of mass of the vesicle ($x_d=0$ on average, and symbolized by ○). Two sinusoidal fits are shown: $y_d=\varrho\sin(\omega t+\phi)$ by the dashed line, and $y_d=\varrho\sin[\omega t+\phi+\epsilon\sin(\omega t)+\epsilon'\cos(\omega t)]$ by the solid line (see the text).

angular velocity versus time can be neglected over three periods. However, it significantly decreases for longer times as detailed below.

B. Determination of stationary angular velocities

The duration of every quarter of period of the rotational motion has been calculated from the positions of maxima, minima, and zeros of $y_d(t)$, leading to instantaneous angular velocities $\omega(t)$ for two vesicles of radius equal to 13.5 and 33.5 μm. It is plotted together with the translational velocity $v(t)$ of the center of mass, for a vesicle with a radius of 13.5 μm, in Fig. 7. Both velocities decrease exponentially before reaching asymptotic values v_∞ and ω_∞. The two displayed curves were fitted by the functions $v-v_\infty=\lambda_v\exp(-t/\tau)$ and $\omega-\omega_\infty=\lambda_\omega\exp(-t/\tau)$. A same relaxation time is found for the two velocities. It is equal to 318 ± 8 and 486 ± 12 s for vesicles with radii 13.5 and 33.5 μm, respectively. Asymptotic values of v_∞ (0.40 and 1.40 μm/s for vesicles of radii 13.5 and 33.5 μm, respectively) lie on the master curve displayed in Fig. 5, which confirms that the stationary regime is reached. The angular

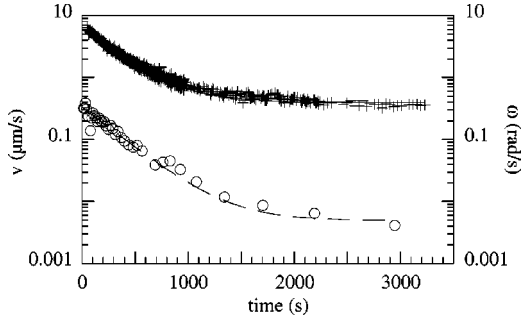

FIG. 7. Variations of translational (v) and angular (ω) velocities vs time t observed on a vesicle of radius 13.5 μm. An exponential fit is superimposed on each curve: Solid line: $v-v_\infty=\lambda_v\exp(-t/\tau)$. Dashed line: $\omega-\omega_\infty=\lambda_\omega\exp(-t/\tau)$.

velocity ω_∞ (0.0050 and 0.0053 rad/s for vesicles of radii 13.5 and 33.5 μm, respectively) is so small that its accurate determination by a direct observation of the stationary state would be hazardous. It is consequently better determined by fitting the relaxation of the transient regime.

The ratio $\omega R/v$ was found to be equal to 0.17 and 0.13 for two vesicles of radii 13.5 and 33.5 μm, respectively. According to Eq. (3), values of $\omega R/v$ are not very sensitive to values of R in the range studied here: with $\delta=48$ nm, the value of this ratio is expected to vary from 0.14 to 0.15 when increasing R from 13.5 to 33.5 μm. These values are close to that observed from experiment. They corroborate the validity of Goldman *et al.*'s model using rigid spheres for describing the vesicles studied here.

This result shows that the vesicles slip at the surface. This slippery motion was not observed by Lorz *et al.* on vesicles under shear flow, probably because of the existence in this study of significant adhering forces wich ensure binding of the vesicle.

VII. MEMBRANE-SUBSTRATE SEPARATION DISTANCE

The above results for rolling motion strongly support the value of δ found from translational velocities measurements and using Eq. (5), i.e., within the rigid sphere approximation. This is the first time, as far as we know, that the separation distance is determined for a moving vesicle.

The value obtained, equal to 48 nm, must be understood in terms of an average value. All the studied vesicles should not have exactly the same δ value, but individual variations of δ around the average are considered to be smaller than the experimental error.

The δ value is of the order of magnitude measured in Ref. [15] with the RICM technique on SOPC vesicles resting on a weakly adhesive substrate. In this work, the absolute separation distance was measured approximately only; it ranges from 31 to 41 nm. Such values of several tens of nanometers for δ may appear surprisingly large. The model developed by Rädler *et al.* to explain their results assumesd that adhesion is controlled by a superposition of three interaction potentials. Two interactions are attractive—van der Waals and gravitational effects—and one is repulsive, the steric interaction arising from the thermally excited out-of-plane fluctuations that repel the membrane from the hard wall. Such a model should also apply for moving vesicles. Although it predicts a strong dependence of the membrane-substrate separation distance with the membrane tension, which was not clearly observed by Rädler *et al.*, this model yields the correct order of magnitude for the membrane-substrate separation distance.

In the case of nonfluctuating and dense spheres, it is simply expected that δ goes to zero, and that the spheres come in contact with the substrate, since van der Waals and gravitational interactions are not counterbalanced by the steric repelling effects. We indeed observed this behavior using micrometric glass beads: they moved irregularly by fits and starts along the inclined plane, likely due to solid friction at the contact of the glass surface. Therefore, although the hydrodynamic behavior of vesicles can be described from that

of rigid spheres, it appears in this study that the vesicle-substrate distance is specific to the soft nature of the membrane and of its large thermal activated fluctuations.

VIII. CONCLUSION

We have studied the sliding and the rolling motion of nondeflated giant vesicles which do not adhere specifically to the substrate. Goldman *et al.*'s frame of description shows that the motion of vesicles is that of nondeformable spheres. The water permeability and the deformability of the membrane do not play active roles in the hydrodynamic behavior of such vesicles. We have determined the thickness of the fluid film between the moving vesicles and the substrate, $\delta = 48$ nm. This value is in qualitative agreement with the current model, which interprets such a large δ value in terms of a balance between van der Waals and gravitational forces and steric repelling forces induced by thermal undulations of the membrane.

An interesting point is to explore whether this framework is valid when the vesicles are deflated and/or adhere to the substrate. Even more interesting will be to explore the migration of vesicles under flow. Indeed, cells and transport vesicles are often submitted to capillary flows in vessels. For instance, many functions of blood leukocytes are dependent of their capacity to adhere to endothelial cells under shear flow [1,18]. A detailed study of vesicle motion close to a wall and submitted to a shear flow is in progress at the moment.

ACKNOWLEDGMENTS

This work was supported by the CNRS through the ''GREPHE'' project. We are very grateful to M. Angelova for sharing her knowledge on experimental aspects, and to C. Misbah for stimulating discussions and encouragement.

[1] O. Tissot *et al.*, Biophys. J. **61**, 204 (1992).
[2] X. Lei, M.B. Lawrence, and C. Dong, J. Biomech. Eng. **121**, 636 (1999); C. Dong and X. Lei, J. Biomech. **33**, 35 (2000).
[3] R. Simson *et al.*, Biophys. J. **74**, 514 (1998).
[4] T.P. Stossel, Science **260**, 1086 (1993).
[5] E. Sackmann, Macromol. Chem. Phys. **195:7**, 28 (1994).
[6] D.G. Swift, R.G. Posner, and D.A. Hammer, Biophys. J. **75**, 2597 (1998).
[7] F.M. Menger and M.I. Angelova, Acc. Chem. Res. **31**, 789 (1998).
[8] F.M. Menger and S.J. Lee, Langmuir **11**, 3685 (1995).
[9] *Handbook of Biological Physics Series, Structure and Dynamics of Membranes*, edited by R. Lipowsky and E. Sackmann (Elsevier, Amsterdam, 1995).
[10] M. Kraus, W. Wintz, U. Seifert, and R. Lipowsky, Phys. Rev. Lett. **77**, 3685 (1996).
[11] I. Cantat and C. Misbah, Phys. Rev. Lett. **83**, 235 (1999).
[12] U. Seifert, Phys. Rev. Lett. **83**, 876 (1999).
[13] B. Lorz, R. Simson, J. Nardi, and E. Sackmann, Europhys. Lett. **51**, 468 (2000).
[14] A.J. Goldman, R.G. Cox, and H. Brenner, Chem. Eng. Sci. **22**, 637 (1967).
[15] J.O. Rädler, T.J. Feder, H.H. Strey, and E. Sackmann, Phys. Rev. E **51**, 4526 (1995).
[16] D. Braun and P. Fromherz, Phys. Rev. Lett. **81**, 5241 (1998).
[17] M. Angelova *et al.*, Prog. Colloid Polym. Sci. **89**, 127 (1992).
[18] D.A. Hammer and S. Apte, Biophys. J. **63**, 35 (1992).